

RESEARCH

Open Access



Flexural Strengthening of RC Columns with Low Longitudinal Steel Ratio using GFRP Bars

Mehdi Esfandi Sarafraz*

Abstract

This research describes the results of an experimental work that aimed to investigate the flexural capacity of RC columns with low longitudinal reinforcement ratio that was strengthened with near surface mounted GFRP bars. The experimental program consisted of four square reinforced concrete columns, including one control specimen that were designed with a longitudinal reinforcement ratio below the minimum required ratio of 1% specified by RC design codes. Three of the four specimens were strengthened with different ratios NSM GFRP bar. The specimens were tested under a combined axial compressive load and lateral cyclic displacement to evaluate this retrofit method for the flexural improvement of RC columns. The efficacy of the proposed strengthening method on the flexural capacity, failure modes, hysteretic curves, energy dissipation capacity, and stiffness are discussed on the basis of the test results. The experimental results demonstrated that the contribution of GFRP bars to the flexural capacity of RC columns was significant. Also, an analytical procedure for calculating the bending moment capacity of RC columns strengthened with GFRP bars subjected to axial and lateral is proposed. The model accuracy is demonstrated by comparing the model predictions with the experimental results. The flexural capacity calculated by this method were in good agreement with the experimental results.

Keywords: RC columns, GFRP rebar, flexural capacity, NSM, seismic strengthening

1 Introduction

Reinforced concrete columns are important elements in the structures. Therefore, their damage leads to the failure of the building. Hence, strengthening of these elements is essential.

Many reinforced concrete columns that were designed and constructed in the last years were designed as gravity columns with minimum longitudinal reinforcement. These columns cannot be able to support sufficient flexural capacity, and they are vulnerable to earthquakes.

Reinforced concrete columns can be seismically deficient in the compressive crushing of concrete, shear, reinforcing bar buckling and flexural strength. Flexural capacity defect in RC columns may occur from the low

ratio of longitudinal steel rebar, corrosion of steel reinforcement or premature cut of the longitudinal steel rebars.

The most common traditional strengthening technique for RC columns with flexural capacity deficiency is including usage of the steel or concrete jacket. This technique is also beneficial in modifying the shear capacity and the ductility of RC columns. But, it may not be feasible due to unfavorable section enlargement, weight increasing, and construction limitation.

In recent years composite materials (FRP) are employed widely to substitute concrete and steel jacket system. The main advantages these systems are their high strength/weight ratio, durability to inappropriate environmental conditions, and simplicity of installation (Saadatmanesh et al. 1994; Nanni and Bradford 1995; Seible et al. 1997; Khalifa et al. 1998). The FRP jacketing can only modify the shear and axial strength of columns through concrete confinement but it cannot enhance the flexural

*Correspondence: sarafraz.m@wtiau.ac.ir
Department of Civil Engineering, West Tehran Branch, Islamic Azad University, Tehran, Iran
Journal information: ISSN 1976-0485 / eISSN 2234-1315

strength of RC columns (Hadi 2006; El Maaddawy 2009), because wrapping the RC column with FRP sheet can only increase the flexural strength by confining effect if compression failure mode accrues (compression concrete reaches its ultimate strain, and steel rebars does not yield).

If the compressive force is very little or the longitudinal steel rebar ratio is less than the minimum ratio in accordance with the RC design codes, the steel rebar will reach yield stress (tension failure mode), and the FRP jacketing is not effective.

Near-surface mounted (NSM) FRP bars are another method that may be employed to enhance the flexural capacity of RC columns. This method includes cutting slits on the surface of the concrete and embedding the FRP bars inside the slits with paste (De Lorenzis and Nanni 2002; Täljsten et al. 2003; Sena-Cruz and Barros 2004; De Lorenzis and Teng 2007). Many studies on NSM FRP bars for reinforced concrete structures have concentrated on flexural retrofitting of beams or slabs (El-Hacha and Rizkalla 2004; Barros and Fortes 2005; Teng et al. 2006), shear retrofitting of RC beam (De Lorenzis and Nanni 2001; Nanni et al. 2004) and flexural retrofitting with prestressed FRP bars (Nordin and Täljsten 2006; Badawi and Soudki 2009; Hajihashemi et al. 2011).

Only a few studies are available that deal with the using NSM FRP bars for increasing flexural capacity of concrete columns. Barros et al. studied eight concrete columns strengthened with NSM bars. These columns tested under combined lateral and axial loading (Barros et al. 2008). Perrone et al. used FRP strips with CFRP sheets to increase the flexural capacity of RC columns (Perrone et al. 2009). El-Maaddawy and El-Dieb used the GFRP NSM bar combined with CFRP jacketing to strengthening the RC columns (El-maaddawy and El-dieb 2011). Bournas and Triantafillou tested eleven rectangular columns strengthened by GFRP, CFRP and steel bars under combined lateral and axial loading. Also, they used FRP jacketing with NSM technique (Bournas and Triantafillou 2009). Sarafraz and Danesh tested rectangular RC columns strengthened by NSM bars and CFRP jacketing under constant axial load and lateral displacement. The test results showed that FRP NSM bars are effective for increasing the flexural strength of RC columns (Sarafraz and Danesh 2010, 2012). Ding et al. developed a retrofitting technique by using BFRP composites with both near surface mounted (NSM) and confinement (Ding et al. 2013). Jiang et al. presented a retrofitting technique using basalt fiber reinforced polymer (BFRP) bars and BFRP jacket for four reinforced concrete circular bridge piers that were damaged in the earthquake. Test results showed that the presented technique is beneficial in strengthening the damaged bridge piers (Jiang et al. 2016).

The main goal of this study is to measure the flexural strengthening of RC columns with low longitudinal reinforcement ratio when strengthened using NSM GFRP bars. The flexural capacity enhancement was attained by embedding NSM GFRP bars in the columns.

To study the efficacy of NSM GFRP bars system, four columns were designed and constructed. The ratio of longitudinal reinforcement was lower than the minimum amount according to the RC design codes (ACI Committee 318 2014). Constant axial compressive loading and cyclic lateral displacement were carried out on both strengthened and unstrengthened specimens.

2 Test Program

2.1 Specimens

Four specimens were built in a similar geometry. The experimental study was based on tests on square columns with cross-section 200 mm, and the clear length equal to 1000 mm. In all specimens, the aspect ratio (effective height to effective depth ratio) is kept constant at 6.57. This ratio was consciously chosen to control the behavior of specimens with the flexural failure rather than the shear failure (Bournas and Triantafillou 2009). The columns were constructed with the reinforced concrete block on top and bottom to apply the axial and lateral loading at the top of the columns and to connect the columns to the supporting frame.

The columns were reinforced with four 10 mm diameter longitudinal rebars located at each corner and with a cover of 25 mm. The longitudinal steel rebar ratio was 0.785%. This is 78% of the minimum reinforcement ratio required by ACI code (ACI Committee 318 2014) to ensure the flexural failure mode of the specimens (fail by yielding of the main steel reinforcement). The transverse reinforcing made from 12 mm diameter spaced 100 mm on center. The detailed information is presented in Table 1 and Fig. 1.

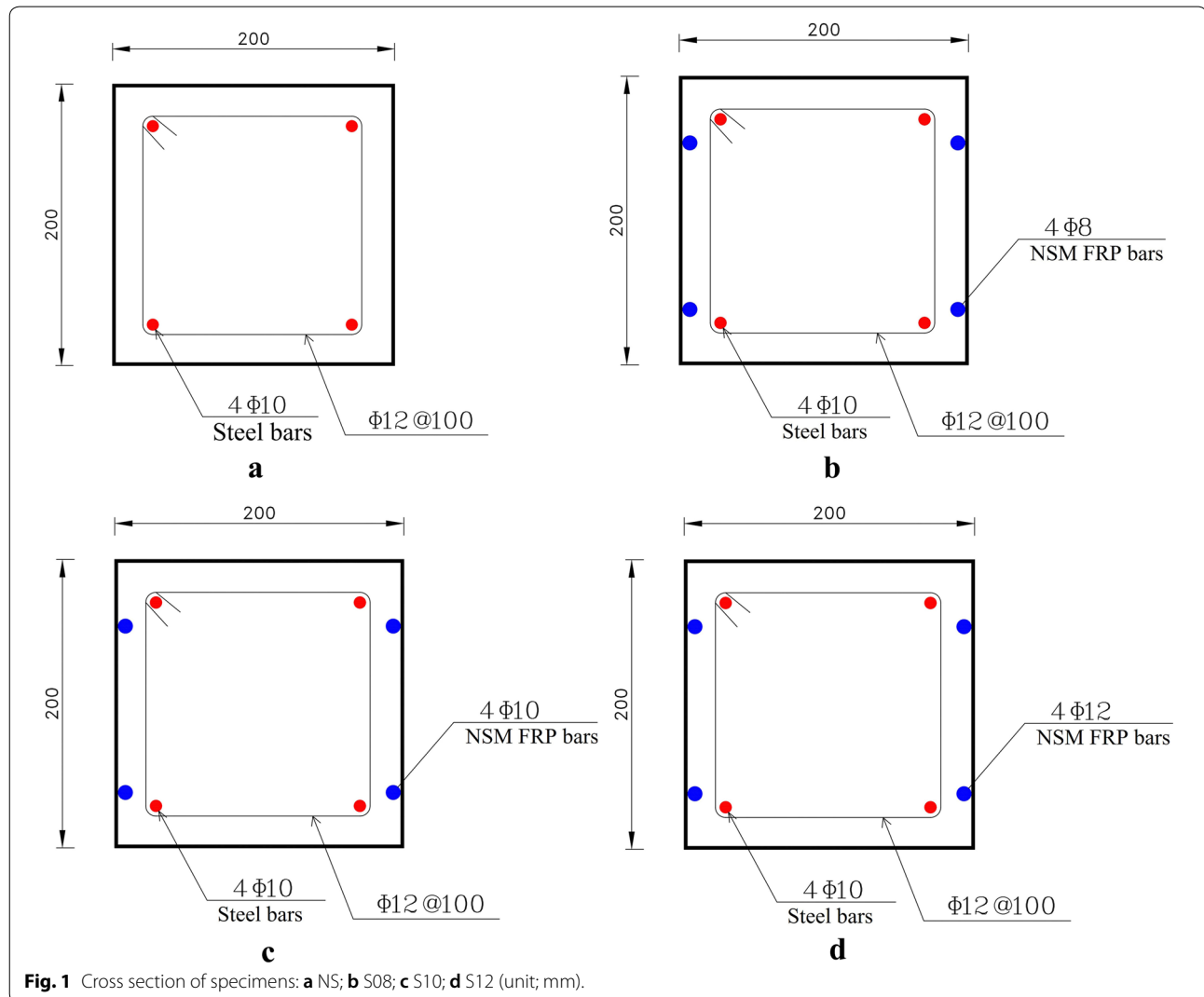
The specimens consist of 4 columns; namely NS, S08, S10 and S12. Column NS was unstrengthened and was tested as the reference column to obtain the strength of the unstrengthened column. Specimens S08, S10, and S12 were strengthened before testing. These columns were constructed by altering the diameter of NSM GFRP bars from 8 to 12 mm.

The column S08 was retrofitted using two GFRP NSM bars with 8 mm diameter embedded on two sides of the specimen. The columns S10 and S12 were strengthened by 10 mm and 12 mm diameter GFRP bars, respectively.

In all columns, the GFRP bars anchored in the bottom block. In this research, the anchorage length of the GFRP bars was not an experimental parameter, and a constant value of 250 mm was initially selected.

Table 1 Properties of specimens.

Specimen	Concrete strength (MPa)	Number of steel rebars	Diameter of steel rebars (mm)	Ratio of steel rebars (%)	Number of GFRP bars	Diameter of GFRP bars (mm)	Ratio of GFRP bars (%)
NS	25.3	4	10	0.785	–	–	–
S08	24.2	4	10	0.785	4	8	0.502
S10	24.8	4	10	0.785	4	10	0.785
S12	25.2	4	10	0.785	4	12	1.13



The details of the retrofitting method are shown in Fig. 1.

2.2 Material Properties

All the specimens were constructed with ready-mixed concrete. The specified strength of concrete was 25 MPa. The strength of the concrete at the time that

specimens were tested, determined on three 150 mm diameter and 300 mm height concrete cylinders, are shown in Table 1. The nominal yield stress of longitudinal and shear steel rebar was 400 MPa. The mechanical characteristics of the epoxy pastes and NSM GFRP bars were specified by the producer and presented in Table 2.

Table 2 Properties of the NSM GFRP bars and epoxy material.

Composite type	Tensile strength (MPa)	Tensile modulus (GPa)	Ultimate strain (%)
GFRP bar	1200	55	2.2
Epoxy mortar	27.6	3	1.4

2.3 NSM Application Procedures

The NSM GFRP bars were inserted in slits that were 1.5d width and depth, which “d” is the diameter of NSM bars. These slits created Along the line of the columns. The dimensions of the slits were selected based on ACI 440.2R-17 (2017). The slits were cleared by compressed air to clean all weak part and dust. The NSM bars were anchored in 250 mm holes were drilled into the bottom block. The anchorage length of the GFRP bars inside the bottom block was selected based on past researches (Barros et al. 2008; Bournas and Triantafillou 2009). The slits and the drilled holes were filled with paste, and the GFRP bars were inserted into the slits and the surface was leveled.

2.4 Test Setup and Loading Protocol

The detail of the test setup is presented in Fig. 2. The test set up included a supporting frame to retain the column, lateral and vertical hydraulic actuator. Specimens were cast on a bottom block to ensure a fixed end. The bottom block was fixed to the supporting frame using high-strength bolts. To prevention of in-plane displacement of the test specimens, side-sway restraint was used. Two hydraulic actuators were applied to exert axial load and lateral displacement.

At the first step, a constant axial compressive load was applied by 500 kN automatic hydraulic actuators and then remained constant. The applied axial compressive load was 200 kN for all columns. This axial load matched to 20% of the ultimate compression capacity of columns.

After that, the lateral load was exerted as displacement control mode by a 250 kN, computer-controlled dynamic actuator to columns under a constant axial force.

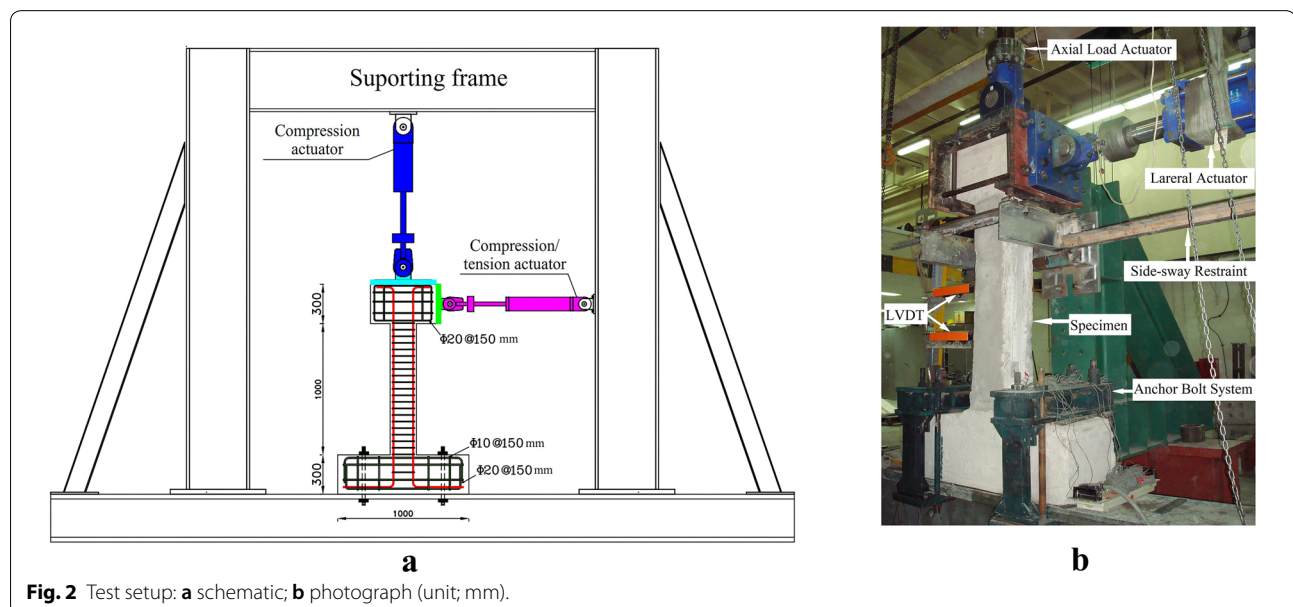
For all specimens, the cyclic displacement level was selected as the coefficient of $0.5\Delta_y$. The yield displacement was calculated numerically for the control specimen NS and held fix for all specimens. In the tests, the lateral displacement rates were chosen as the ratio of 5 mm. The lateral loading consisted of three cycles at each displacement level to detect the strength and stiffness degradation specification.

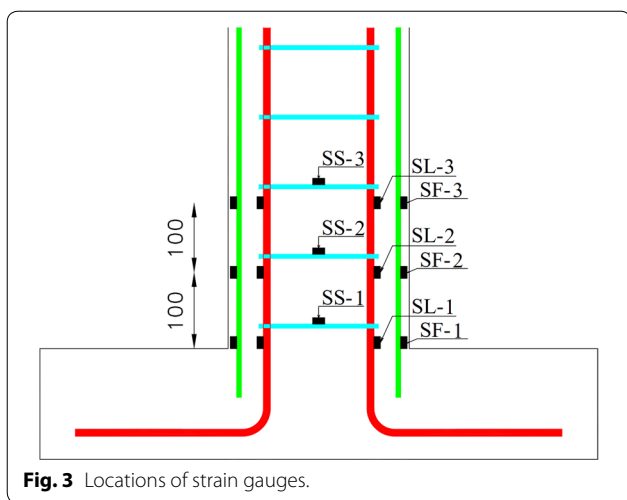
2.5 Instrumentation

The strains of GFRP bars, steel reinforcement, and the horizontal displacements of the column were recorded during the testing.

Instruments including strain gauges and LVDTs were employed. Strains in the GFRP bar and steel reinforcement were recorded using strain gauges. Three strain gauges were bonded at the bottom of each GFRP bars. Also, three strain gauges were bonded on longitudinal reinforcement, and one strain gauges were bonded on three ties. The positions of strain gauges are displayed in Fig. 3.

Column cyclic displacement was recorded at the 1000 mm distance from the bottom block with LVDT. Also, two LVDTs were placed to measure the horizontal movement of the bottom block.





3 Experimental Results

3.1 Test Results and Observation

The main target in this research was to evaluate the influence of GFRP bars for the flexural strengthening of RC columns with low longitudinal steel rebar ratio, so the response of all specimens due to the low ratio of longitudinal reinforcement was controlled by bending.

In the control specimen NS, first flexural crack observed at the interval of 50 mm on the tension face at the early stages of loading and then other flexural cracks were seen. These cracks were concentrated around the base of the column. At the lateral displacement of 19.8 mm, the lateral load reached the maximum and concrete crushing began. The first tensile reinforcement yielded at the lateral displacement of 7.2 mm, and after that, the cracks on the base of the column were opened extensively. The concrete cover spalled at the displacement of 26.7 mm. The column loosed and sharply defective at the lateral displacement of 40.1 mm. The test was

finished with severe spalling and crushing of the concrete and buckling of the main rebars as shown in Fig. 4a.

All strengthened specimens showed similar behavior in cracking pattern and failure mechanism. These specimens failed in flexure due to their high value of the aspect ratio, low ratio of longitudinal reinforcement, and the high ratio of shear reinforcement. These columns failed by the cracking the epoxy paste concurrent with the debonding of the GFRP bars and separation of the covers of the NSM GFRP bars as shown in Fig. 4b. Steel bar buckling always happened suddenly after the failure of the NSM bars. All strengthened columns displayed higher flexural strength compared to the control specimen NS. The failure mechanism for all strengthened specimens was because of the failure of the NSM bars at the column base, as shown in Fig. 4c.

For specimen S08, the first flexural crack observed at the base of the column at the lateral displacement of 3.7 mm and then other cracks were propagated along the height of the column. At the lateral displacement of 6.3 mm, the cracking noise of epoxy paste was heard. The lateral strength reached the peak value at the displacement of about 20.3 mm and the tensile steel rebars began to yield. The fracture of epoxy paste occurred at the displacement of 33.7 mm and the lateral load capacity decreased suddenly at this moment. The failure mode included the development of horizontal, and vertical cracks in epoxy paste and concrete, bond failure and buckling of GFRP bars followed by concrete crushing at the column base.

For specimen S10, horizontal flexural cracks observed on the tensile side at the base of the specimen at the lateral displacement of 4.5 mm. When the lateral displacement reached to 6.6 mm, the breaking noise of epoxy paste was heard and then a crack created at the interface between the epoxy paste and GFRP bar. At the lateral



displacement of 19.8 mm, the first steel rebar started to yield. The lateral strength reached the peak value at the displacement of about 20.6 mm. The failure of the epoxy paste happened at the displacement of 35.6 mm. The failure process included the development of splitting cracks in the epoxy paste, and bond failure of GFRP bars followed by concrete crushing at the column base. In this time, the load sharply decreased.

For specimen S12, first flexural cracking observed at the lateral displacement of 4.5 mm. At the lateral displacement of 6.8 mm, the crackling sound of epoxy paste was heard. At the lateral displacement of 10.6 mm, flexural cracks propagated along the height of the column at the distance of 180 mm from the top of the base. The lateral strength reached the peak value at the displacement of about 24.6 mm. At the same time, yielding of the main tensile steel reinforcement started. In the following, the epoxy cover was split, intersected by the cracks, and debonding between the GFRP bars and epoxy paste occurred. In this case, many cracks were created in the epoxy paste around the specimen base, and the other part of the epoxy paste remained intact. At the lateral displacement of 38.6 mm, a breaking noise was heard that demonstrated the failure of epoxy paste, and the lateral strength dropped suddenly.

3.2 Force–Displacement Curves

Table 3 summarizes both the positive and negative maximum lateral load capacity, the displacement equivalent to the maximum load and the increase rate in the lateral strength of the specimens. The lateral load–displacement hysteresis curves are shown in Fig. 5. These curves are configured to show maximum strength in the positive direction. In control specimen NS, a pinching effect of the hysteresis curve happened. Also, retrofitted specimens displayed a slight pinching effect after reaching peak strength. In the retrofitted specimens this pinching effect was decreased, because of the enhancement in the flexural capacity generated by the GFRP bars. The pinching seen in the hysteresis curves in retrofitted specimens is due to slip between the GFRP bars and the surrounding paste inside the slits

and the linear elastic behavior of the GFRP bars. Also, the buckling of GFRP bars led to a pinching effect in hysteretic curves.

It is clear that the strength of all specimens was significantly reduced after reaching peak strength. The bond failure between GFRP bars and epoxy paste resulted in a drop of strength. Since the GFRP bar cover is small and the amount of force in GFRP bar is high, tensile splitting cracks develop in the surrounding paste in the radial direction and led to premature bond failure (Harajli 2009). Cracking in the epoxy paste and debonding of the GFRP bars lead to decrease the lateral strength capacity in the next cycle. To prevent debonding of FRP NSM bars, it is recommended to jacket the column with FRP sheet (El-maaddawy and El-dieb 2011; Bournas and Triantafillou 2009; Sarafraz and Danesh 2010, 2012). In all strengthened specimens, flexural capacity increases impressively. Compared to the specimen NS, the lateral capacity in S08, S10 and S12 attained the peak at the displacement of 20.3 mm, 20.6 mm and 24.6 mm, and the maximum strength increased up to approximately 20%, 35% and 44% than that of control specimen, respectively.

In all specimens, the negative and positive peak strength values were not equal. This matter demonstrated that the steel rebars in the columns were not exactly symmetrical and so, the effective depth of steel reinforcement is different in each direction.

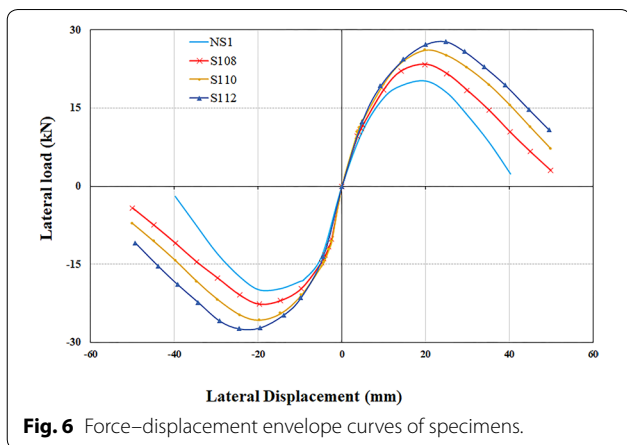
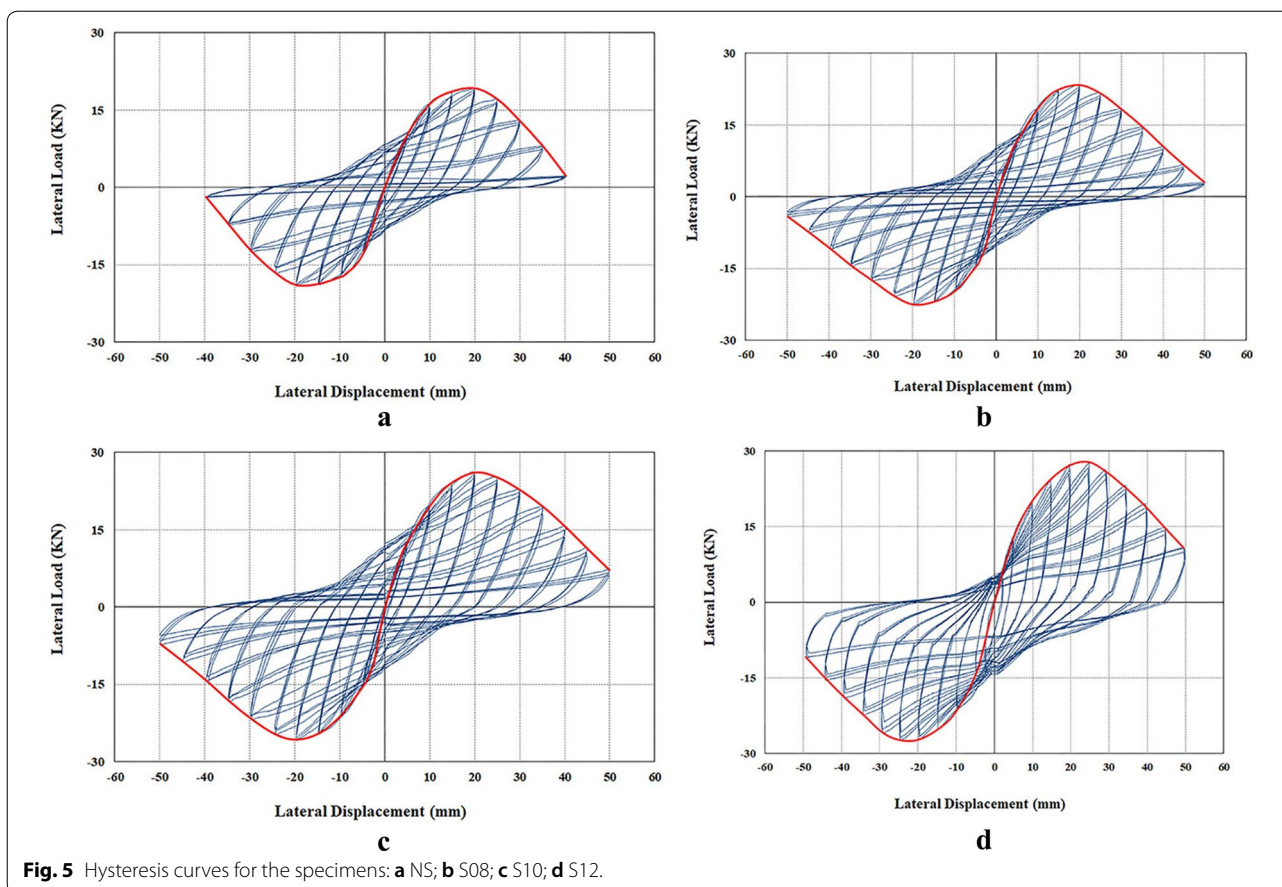
All strengthened specimens failed at a load and displacement more than control specimen. In strengthened specimens, the increasing the NSM reinforcing ratio by 125% (12 mm diameter versus 8 mm diameter) Increases the lateral strength up to 44% and 20%, respectively.

Figure 6, demonstrates the envelop curves for all columns obtain from the hysteresis loops. As can be seen from Fig. 6, and Table 3, in columns that retrofitted with more GFRP bar ratio, the flexural capacity improved when compared to the similar specimen retrofitted with less GFRP bar ratio. So, increasing the ratio of NSM bars increased the column’s flexural capacity.

Table 3 Lateral load–displacement parameters.

Specimen	Peak force, (kN)			Increase in peak force (%)	Displacement at peak force, (mm)			Bending moment, (KN m)		
	P ⁺ _{peak}	P ⁻ _{peak}	Average		Δ ⁺ _{peak}	Δ ⁻ _{peak}	Average	Experimental	Analytical	Error ^a (%)
NS	19.21	- 18.94	19.07	-	19.87	- 19.72	19.79	21.9	24.1	9.8
S08	23.41	- 22.58	22.99	20	20.22	- 20.48	20.35	26.4	28.2	6.6
S10	26.12	- 25.69	25.90	35	20.81	- 20.53	20.67	29.8	31.3	5.1
S12	27.85	- 27.34	27.59	44	24.72	- 24.58	24.65	31.7	34.4	8.4

^a Error (%) = (M_{Analytical} - M_{Experimental}) / M_{Experimental} × 100.

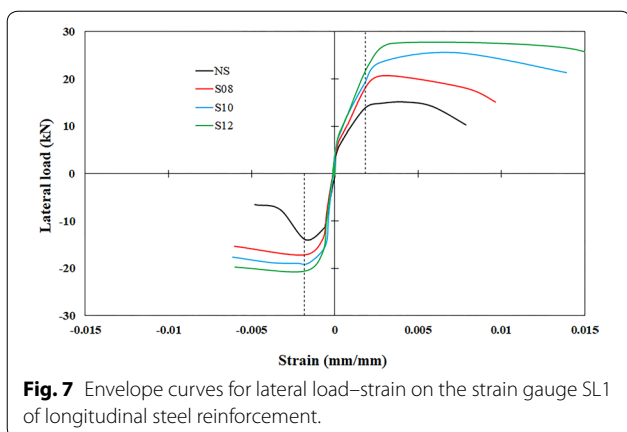


3.3 Strains in GFRP Bars and Steel Reinforcement

Based on the results from the strain gauges glued to the steel reinforcement at various locations, the longitudinal steel rebars of all columns yielded. The smooth envelope curves of lateral load versus the strain recorded in the strain gauge SL1 attached to the main steel bars (see Fig. 3) are given in Fig. 7. The strains in the longitudinal

steel reinforcements in strengthened specimens are smaller than the strains in the control column, and therefore, the yielding of longitudinal steel reinforcement in strengthened specimens occurred later compared with control specimen. Therefore, GFRP bars can contribute to decreasing the strain and stress in the longitudinal steel reinforcement.

Figure 8 shows the curves of the lateral displacement versus the strains measured in the strain gauge SF2 attached to the GFRP bars (see Fig. 3), for the strengthened specimens. The recorded strains in GFRP bars were nearly small before reach to peak strength but increased as soon as yielding the main steel reinforcement occurred. The bond-slip failure between the GFRP bars and the surrounding epoxy paste in S08, S10, and S12 started when the average tensile strain in GFRP bars were about 1.05%, 0.95%, and 0.9%, respectively. According to Fig. 8, it is observed that the GFRP bars strains remain constant or reduces while the displacement levels are increasing in the cyclic loading. It is due to debonding effects at the GFRP bar–epoxy paste or the epoxy paste–concrete surface interface. Due to the cracking the epoxy paste and partial debonding of the GFRP bars, the maximum recorded strain in the GFRP bars was about



48–57% of ultimate strain based on Table 2. The strain values measured in the GFRP bars illustrate that GFRP bars contribute to load carrying capacity and are effective for lateral load enhancement of RC columns.

According to Fig. 8, it is clear that the compressive strain in the GFRP bars is less than the tensile strain in the same cycle. It is due to the effect and contribution of the concrete and epoxy paste conjunct the GFRP bars in compression loads. This demonstrates that the GFRP bars in both the tension and compression side of the column were effective in lateral load capacity.

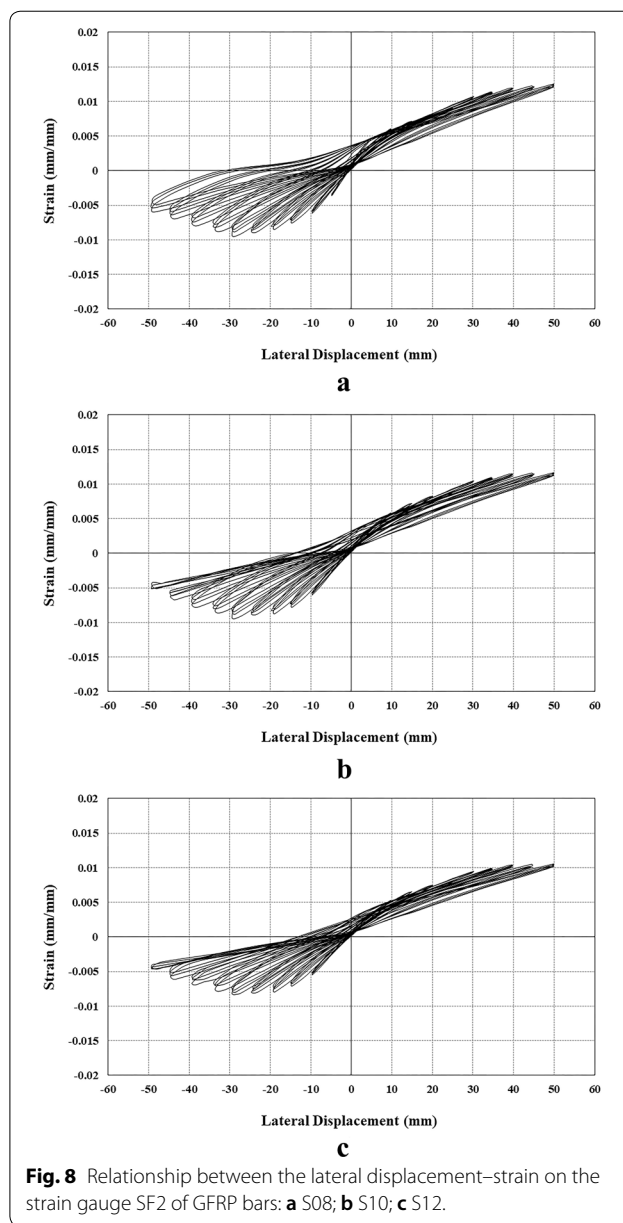
3.4 Dissipated Energy Capacity

The dissipated energy capacity is an important parameter for evaluation of the seismic efficiency of structural elements. The dissipated energy capacity of the specimens is determined by the area enclosed by the lateral load–deformation hysteretic curve for each loading cycle.

The summation of the areas of the hysteretic loops at different cycles is the cumulative energy dissipation. Wider hysteresis loops indicate higher dissipated energy capacity. Figure 9 presents the dissipated capacity versus lateral displacement.

As illustrated in Fig. 9, and Table 4, the cumulative dissipated energy of the retrofitted specimens, was about 170–260% greater than un-retrofitted specimen NS. This matter demonstrates that the strengthened specimens have more energy dissipation capacity, and this capacity increases with the increase of NSM rebar ratio. So, increasing the number of NSM bar increases the dissipated energy capacity.

The results of energy dissipation showed that the strengthening methods could increase the toughness and the energy dissipation capacity of columns and hence, is beneficial for strengthening of reinforced concrete columns.



3.5 Stiffness Degradation

During the reversed cycle loading, the stiffness and strength of reinforced concrete columns decrease after concrete crushing and reinforcement yielding.

Figure 10, illustrates the variation of stiffness degradation (K_i/K_0) with the lateral displacement for all specimens, in which K_0 is the initial stiffness, K_i is the secant stiffness at a given displacement, and (K_i/K_0) is the percentage of residual stiffness.

As demonstrated in Fig. 10, all specimens had similar stiffness degradations before reaching the ultimate load carrying capacity. After reaching the maximum lateral load, the stiffness degradation was commonly alike

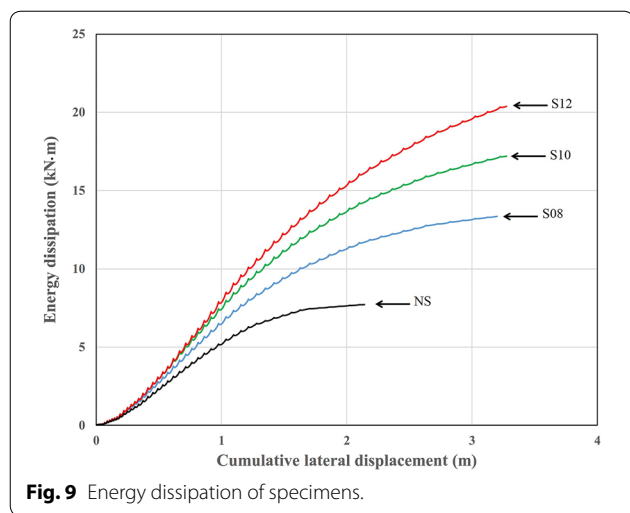


Fig. 9 Energy dissipation of specimens.

Table 4 Energy dissipation results

Specimen	Energy dissipation (kN m)	Increase in energy dissipation (%)
NS	7.71	–
S08	13.41	74
S10	17.19	122
S12	20.37	164

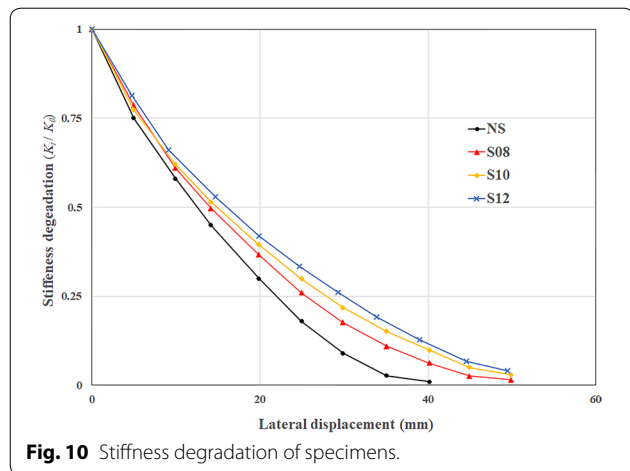


Fig. 10 Stiffness degradation of specimens.

between all the retrofitted specimens and was slower than the control specimen. This is due to the severe failure and crushing in the compression side of the control column after reaching the peak strength as compared with strengthened specimens. Therefore, all the retrofitted specimens displayed better strength degradation

compared with the control column. Also, it is observed that stiffness degradation was similar in all specimens before reaching the ultimate load carrying capacity. Therefore, it is clear that the strengthening method slowed down the deterioration of the force–displacement curve in softening branch.

4 Analytical Calculations

In this section, an analytical procedure has presented to calculate the bending moment capacity of RC columns retrofitted with NSM FRP bars under axial load via classic analysis method developed for reinforced concrete columns based on strain compatibility and force equilibrium (ACI Committee 318 2014). For this purpose, the concrete strain at failure is assumed, and the depth of the neutral axis is calculated by trial and error method. The analysis assumptions according to the ACI code (ACI Committee 318 2014) are as follows: (a) plane sections stay plane after bending, (b) strains in concrete, GFRP bars, and steel reinforcement are proportional to the distance from the neutral axis, (c) tensile strength of concrete can be ignored, (d) the maximum axial strain in compression concrete is 0.003 mm/mm, (e) the stress–strain behavior for steel rebars is elastic perfect plastic, (f) the stress–strain behavior for NSM FRP bar is linear elastic, and (g) NSM FRP bars and steel reinforcements are effective in tension and compression. Figure 11 shows the strain compatibility and force equilibrium conditions. The analytical procedure used to evaluate the bending moment capacity of RC columns is achieved as follows:

- For a given axial compression load, the depth of the neutral axis, c , is assumed.
- The strain of concrete, steel reinforcement, and GFRP bars are calculated utilizing the strain compatibility of the section.
- The stress of concrete, steel reinforcement, and GFRP bars are calculated based on the constitutive laws of the Materials.
- The neutral axis depth for a given axial compression load is calculated from the equilibrium, as follows:

$$c = \frac{P + A_s f_s - A'_s f'_s + A_{NSM} f_{NSM} - A'_{NSM} f'_{NSM}}{0.85 \beta_1 f'_c b} \tag{1}$$

- If the determined amount of the neutral axis, c , is different from the assumed one, another amount assumes and the procedure is continued until the two amount is matched. The bending moment capacity of the column is calculated as follows:

$$\begin{aligned}
 M_n = & 0.85 \beta_1 f'_c bc \left(\frac{h}{2} - \frac{\beta_1 c}{2} \right) \\
 & + A_s f_s \left(d_s - \frac{h}{2} \right) + A'_s f'_s \left(\frac{h}{2} - d'_s \right) \\
 & + A_{NSM} f_{NSM} \left(\frac{h}{2} - d'_{NSM} \right) \\
 & + A'_{NSM} f'_{NSM} \left(\frac{h}{2} - d'_{NSM} \right)
 \end{aligned} \tag{2}$$

The analytical procedure was implemented in a simple computer program based on Microsoft Excel. The bending moment capacities were calculated for all specimens and are presented in Table 3. According to Table 3, it is clear that the analytical procedure gives suitable predictions for the bending moment capacity of RC columns that retrofitted with GFRP bars. The difference between the analytical and experimental results may be due to a variation in the properties of the materials and debonding of GFRP bars. All calculated bending moment is within a 10% error band, which shows the accuracy and reliability of the proposed method in determining the bending moment capacity of RC columns under axial and lateral loading.

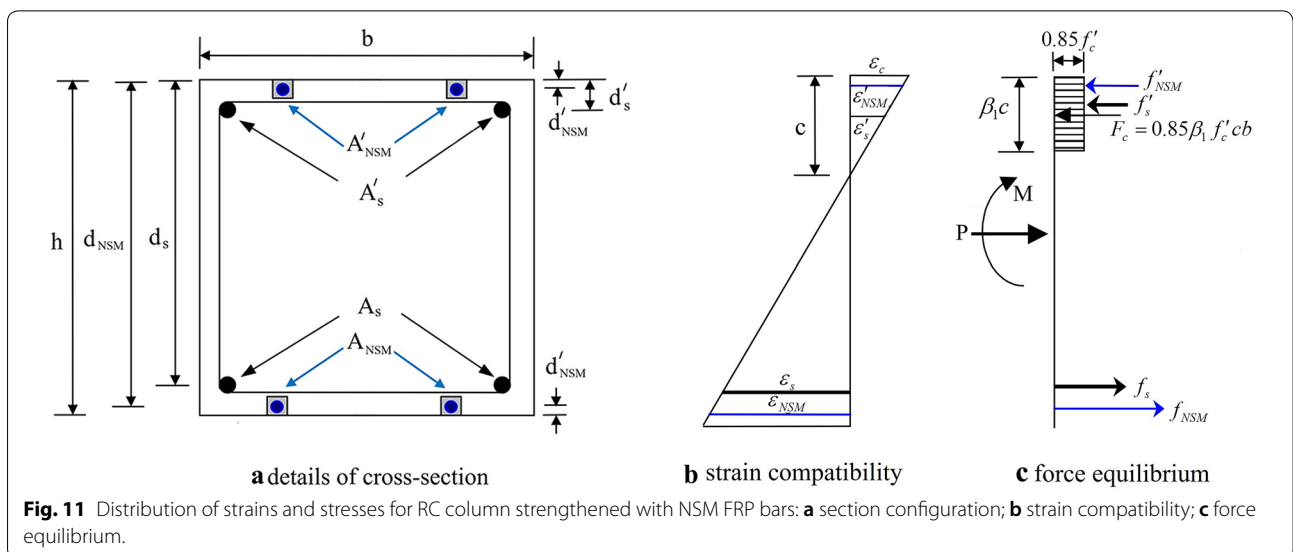
5 Summary and Conclusions

The main idea of this research was to study the use of GFRP bars to modify the flexural capacity of RC columns with low longitudinal reinforcement ratio.

Four square RC columns were built and subjected to the axial load and cyclic lateral displacement. All specimens were built with low longitudinal reinforcement ratio (0.785%). Also, an analytical method for calculating

the bending moment capacity of RC columns retrofitted with GFRP bar was proposed. According to the experimental outcomes, the following results are obtained:

1. The proposed strengthening method is effective for enhancement of the flexural strength of RC columns containing low longitudinal reinforcement ratio under axial and lateral loading.
2. The specimens with a larger diameters GFRP bars show a greater lateral load capacity. Since the ratio of steel reinforcement is the same for all specimens, the flexural capacity of the strengthened columns can increase with increasing the ratio of NSM FRP bars.
3. Due to the cracking the epoxy paste and bond failure between GFRP bars and epoxy paste, the maximum recorded strain in the GFRP bars was below ultimate strain. So, the behavior of the interface between GFRP bar–epoxy paste and the epoxy paste–concrete surface can determine the performance of the retrofitted specimen.
4. The hysteretic curves of strengthened specimens had pinching due to bond slip between the GFRP bars and the surrounding paste inside the slits and the linear elastic behavior of the GFRP bars.
5. The increasing of the NSM GFRP bar ratio can improve the dissipated energy capacity.
6. NSM GFRP bar could be used to delay the stiffness degradation of the RC columns. After reaching peak load, the stiffness degradation of retrofitted specimens was slower than the unretrofitted specimens.
7. The proposed analytical method is capable of predicting the bending moment capacity of RC columns retrofitted with GFRP bar with sufficient accuracy.



List of symbols

A_{NSM} : cross section area of tensile NSM FRP bar (mm^2); A'_{NSM} : cross section area of compressive NSM FRP bar (mm^2); A_s : cross section area of tensile steel reinforcement (mm^2); A'_s : cross section area of compressive steel reinforcement (mm^2); b : width of column (mm); c : depth of neutral axis measured from extreme compression fiber (mm); d_{NSM} : depth to tension NSM FRP bar centroid (mm); d'_{NSM} : depth to compression NSM FRP bar centroid (mm); d_s : depth to tension steel reinforcement centroid (mm); d'_s : depth to compression steel reinforcement centroid (mm); F_c : total compression force of concrete (N); f'_c : Compressive strength of concrete (MPa); f_{NSM} : stress in tension NSM FRP bar (MPa); f'_{NSM} : stress in compression NSM FRP bar (MPa); f_s : stress in tension steel reinforcement (MPa); f'_s : Stress in compression steel reinforcement (MPa); h : height of column (mm); K_0 : initial stiffness (N/m); K_1 : secant stiffness (N/m); M_n : nominal bending moment capacity (N.mm); P : axial compression load on column (N); β_1 : ratio of depth of equivalent rectangular stress block to depth of the neutral axis; ϵ_c : compressive strain in the concrete (mm/mm); ϵ_{NSM} : strain in tension NSM FRP bar (mm/mm); ϵ'_{NSM} : strain in compression NSM FRP bar (mm/mm); ϵ_s : strain in tension steel reinforcement (mm/mm); ϵ'_s : strain in compression steel reinforcement (mm/mm).

Acknowledgements

The author would like to appreciate the structural laboratory at the international institute of earthquake engineering and Seismology (IIEES) for testing and CSM company for construction the specimens.

Authors' contributions

MES performed literature review, designed the specimens, performed experiments, and write the manuscript. The author read and approved the final manuscript.

Funding

The costs of construction of specimens and tests were paid by the CSM company (A local company) for the development of science. This company does not have any claims about the results.

Availability of data and materials

Please contact author for data requests.

Competing interests

The author confirms that he has read SpringerOpen's guidance on competing interests and has included these in the manuscript.

Received: 7 August 2018 Accepted: 21 June 2019

Published online: 08 August 2019

References

- ACI 440.2R-17. (2017). Guide for the design and construction of externally bonded FRP systems for strengthening concrete structures.
- ACI Committee 318. (2014). Building code requirements for structural concrete (ACI 318M-14).
- Badawi, M., & Soudki, K. (2009). Flexural strengthening of RC beams with prestressed NSM CFRP rods—Experimental and analytical investigation. *Construction and Building Materials*, 23, 3292–3300.
- Barros, J. A. O., & Fortes, A. S. (2005). Flexural strengthening of concrete beams with CFRP laminates bonded into slits. *Cement & Concrete Composites*, 27, 471–480.
- Barros, J. A. O., Varma, R. K., Sena-Cruz, J. M., & Azevedo, A. F. M. (2008). Near surface mounted CFRP strips for the flexural strengthening of RC columns: Experimental and numerical research. *Engineering Structures*, 30, 3412–3425.
- Bournas, D. A., & Triantafyllou, T. C. (2009). Flexural strengthening of reinforced concrete columns with near-surface-mounted FRP or stainless steel. *ACI Structural Journal*, 106, 495–505.
- De Lorenzis, L., & Nanni, A. (2001). Shear strengthening of reinforced concrete beams with near-surface mounted fiber-reinforced polymer rods. *ACI Structural Journal*, 98, 60–68.
- De Lorenzis, L., & Nanni, A. (2002). Bond between near surface mounted FRP rods and concrete in structural strengthening. *ACI Structural Journal*, 99, 123–133.
- De Lorenzis, L., & Teng, J. G. (2007). Near-surface mounted FRP reinforcement: An emerging technique for strengthening structures. *Composites Part B Engineering*, 38, 119–143.
- Ding, L., Wu, G., Yang, S., & Wu, Z. (2013). Performance advancement of RC columns by applying basalt FRP composites with NSM and confinement system. *Journal of Earthquake and Tsunami*, 7, 1350007-1–1350007-20.
- El Maaddawy, T. (2009). Strengthening of eccentrically loaded reinforced concrete columns with fiber-reinforced polymer wrapping system: Experimental investigation and analytical modeling. *Journal of Composites for Construction*, 13, 13–24.
- El-Hacha, R., & Rizkalla, S. H. (2004). Near-surface-mounted fiber-reinforced polymer reinforcements for flexural strengthening of concrete structures. *ACI Structural Journal*, 101, 717–726.
- El-Maaddawy, T., & El-Dieb, A. S. (2011). Near-surface-mounted composite system for repair and strengthening of reinforced concrete columns subjected to axial load and biaxial bending. *Journal of Composites for Construction*, 67, 602–614.
- Hadi, M. N. S. (2006). Behaviour of FRP wrapped normal strength concrete columns under eccentric loading. *Composite Structures*, 72, 503–511.
- Hajihashemi, A., Mostofinejad, D., & Azhari, M. (2011). Investigation of RC beams strengthened with prestressed NSM CFRP laminates. *Journal of Composites for Construction*, 15, 887–895.
- Harajli, M. H. (2009). Bond strengthening of lap spliced reinforcement using external FRP jackets: An effective technique for seismic retrofit of rectangular or circular RC columns. *Construction and Building Materials*, 23, 1265–1278.
- Jiang, S.-F., Zeng, X., Shen, S., & Xu, X. (2016). Experimental studies on the seismic behavior of earthquake-damaged circular bridge columns repaired by using combination of near-surface-mounted BFRP bars with external BFRP sheets jacketing. *Engineering Structures*, 106, 317–331.
- Khalifa, A., Gold, W. J., Nanni, A., & Abdel Aziz, M. I. (1998). Contribution of externally bonded FRP to shear capacity of RC flexural members. *Journal of Composites for Construction*, 2, 195–202.
- Nanni, A., & Bradford, N. M. (1995). FRP jacketed concrete under uniaxial compression. *Construction and Building Materials*, 9, 115–124.
- Nanni, A., Di Ludovico, M., & Parretti, R. (2004). Shear strengthening of a PC bridge girder with NSM CFRP rectangular bars. *Advances in Structural Engineering*, 7, 297–309.
- Nordin, H., & Täljsten, B. (2006). Concrete beams strengthened with prestressed near surface mounted CFRP. *Journal of Composites for Construction*, 10, 60–68.
- Perrone, M., Barros, J. A. O., & Aprile, A. (2009). CFRP-based strengthening technique to increase the flexural and energy dissipation capacities of RC columns. *Journal of Composites for Construction*, 13, 372–383.
- Saadatmanesh, H., Ehsani, M. R., & Li, M. W. (1994). Strength and ductility of concrete columns externally reinforced with fiber composite straps. *ACI Structural Journal*, 91, 434–447.
- Sarafraz, M., & Danesh, F. (2010). Experimental study on flexural strengthening of RC columns with near surface mounted FRP bars. *Journal of Seismology and Earthquake Engineering*, 12, 39–50.
- Sarafraz, M. E., & Danesh, F. (2012). New technique for flexural strengthening of RC columns with NSM FRP bars. *Magazine of Concrete Research*, 64, 151–161.
- Seible, F., Priestley, M. J. N., Hegemier, G. A., & Innamorato, D. (1997). Seismic retrofit of RC columns with continuous carbon fiber jackets. *Journal of Composites for Construction*, 1, 52–62.
- Sena-Cruz, J., & Barros, J. A. O. (2004). Bond between near-surface mounted carbon-fiber reinforced polymer laminate strips and concrete. *Journal of Composites for Construction*, 8, 519–527.
- Täljsten, B., Carolin, A., & Nordin, H. (2003). Concrete structures strengthened with near surface mounted reinforcement of CFRP. *Advances in Structural Engineering*, 6, 201–213.
- Teng, J. G., De Lorenzis, L., Wang, B., Li, R., Wong, T. N., & Lam, L. (2006). Debonding failures of RC beams strengthened with near surface mounted CFRP strips. *Journal of Composites for Construction*, 10, 92–105.

Publisher's Note

Springer Nature remains neutral with regard to jurisdictional claims in published maps and institutional affiliations.